Journal of Alloys and Compounds 594 (2014) 148–152

Contents lists available at ScienceDirect

Journal of Alloys and Compounds

journal homepage: www.elsevier.com/locate/jalcom

A neutron diffraction study of the $R_{15}Ge_9C$ compounds (R = Ce, Pr, Nd)

S. Tencé [a,b,c,*], O. Isnard [a,b], F. Wrubl [d], P. Manfrinetti [d,e]

[a] Université Grenoble Alpes, Institut Néel, BP166, F-38042 Grenoble, France
[b] CNRS, Institut Néel, Rue des Martyrs, F-38042 Grenoble, France
[c] Institut de Chimie de la Matière Condensée de Bordeaux (ICMCB), Université de Bordeaux, 87 Avenue Docteur Albert Schweitzer, 33608 Pessac Cedex, France
[d] Department of Chemistry, University of Genoa, Via Dodecaneso 31, 16146 Genoa, Italy
[e] Institute SPIN – CNR, Corso Perrone 24, 16152 Genoa, Italy

ARTICLE INFO

Article history:
Received 7 November 2013
Received in revised form 9 January 2014
Accepted 16 January 2014
Available online 24 January 2014

Keywords:
Rare earth interstitial carbides
Crystal superstructure
Neutron diffraction
Magnetic structure

ABSTRACT

In this work we report the results of the neutron diffraction investigation performed on the germanides $R_{15}Ge_9C$, for R = Ce, Pr and Nd ($La_{15}Ge_9Fe$-type, *hP*50, $P6_3mc$, $Z = 2$), to refine the crystal superstructure of these compounds and determine their magnetic structures. The interstitial carbon atoms occupy mainly the 2*b* Wyckoff site in the position (1/3 2/3 ~1/2) and also, with a smaller occupancy rate, the Wyckoff site 2*a* at (0 0 ~1/2). In the magnetic state, the three compounds display predominantly a ferromagnetic behavior with the propagation vector **k** = [000]. These results are in agreement with the magnetization measurements, with $T_C = 10$, 30 and 80 K as Curie temperature of $Ce_{15}Ge_9C$, $Pr_{15}Ge_9C$ and $Nd_{15}Ge_9C$, respectively. $Ce_{15}Ge_9C$ and $Nd_{15}Ge_9C$ present a ferromagnetic alignment of the R moments along the *c*-axis and an antiferromagnetic spin arrangement within the (*a*–*b*) plane. For $Pr_{15}Ge_9C$ the ferromagnetic contribution is found within the (*a*–*b*) plane, as previously observed for the isotypic compound $Tb_{15}Si_9C$. The carbides crystal structure possesses four inequivalent rare earth sites carrying different magnetic moments, leading to mean values of 0.9 μ_B/Ce, 1.1 μ_B/Pr and 2.2 μ_B/Nd for $Ce_{15}Ge_9C$, $Pr_{15}Ge_9C$ and $Nd_{15}Ge_9C$, respectively.

The magnetic structures of these $R_{15}Ge_9C$ compounds differ strongly from those of their parent R_5Ge_3 germanides, but present strong similarities with the structures of the $R_{15}Si_9C$ compounds. The overall results indicate and confirm the drastic influence of carbon insertion in the rare earth environment.

1. Introduction

It has been shown that intermetallic compounds $La_{15}Ge_9Z$, where Z is an interstitial element (Z = C, Mn, Fe, Co, Ni, Cu, Ru, O, P), could be synthesized [1]. This results from a remarkable feature of R_5X_3 intermetallic phases (R = rare-earth) which can accommodate such a variety of elements interstitially in the centers of the antiprisms to produce filled versions of the same structure type. The obtained superstructure, $La_{15}Ge_9Fe$-type (*hP*50, $P6_3mc$, $Z = 2$), is strictly related with the parent arrangement of the R_5X_3 intermetallics crystallizing in the hexagonal Mn_5Si_3 type structure (*hP*16, $P6_3/mcm$, $Z = 2$). Indeed, this superstructure contains octahedral cavities, formed by the R atoms, in which small atomic species can be inserted. Recently, this family has been extended, with carbon as interstitial element, to the silicides $R_{15}Si_9C$ with heavy lanthanides and to the germanides $R_{15}Ge_9C$ for R = Ce, Pr and Nd [2,3]. These results showed that C insertion significantly modifies the magnetic properties of the parent R_5X_3 compounds. Here we concentrate on the isotype $R_{15}Ge_9C$ germanide compounds which have been reported to form with Ce, Nd and Pr but not with Sm or Gd. For these last two rare earth elements which do not form the superstructure, simpler $R_5X_3C_{0.33}$ stuffed phases has been observed [3]. In this latter structure, the C atoms randomly occupy both available 2*b* octahedral cavities formed by the 6gR atoms, up to the maximum extent ($x = 1$). On the contrary, in the triple cell of the stoichiometric $R_{15}X_9C$, only one-third of all the six available cavities per unit cell are occupied (as indicated by the stoichiometric formula), and the insertion takes place in an ordered fashion.

The article is devoted to the investigation of the crystal and magnetic structure of the $R_{15}Ge_9C$ germanide compounds (R = Ce, Pr, Nd) from high resolution neutron powder diffraction. Indeed, neutron scattering not only enables to determine the magnetic ordering but also offers the advantage to be sensitive to light elements like carbon atoms. The article is organized as follows, in the next section the sample synthesis and the neutron diffraction details are described, then the Section 3 presents the results starting from the description of the crystal structure followed by the successive discussion of the magnetic structure obtained for

* Corresponding author. Address: ICMCB – CNRS UPR9048, 87 Avenue du Docteur Schweitzer, 33608 Pessac Cedex, France. Tel.: +33 (0)540006678.
E-mail address: tence@icmcb-bordeaux.cnrs.fr (S. Tencé).

http://dx.doi.org/10.1016/j.jallcom.2014.01.115
0925-8388/

$Nd_{15}Ge_9C$, $Pr_{15}Ge_9C$and $Ce_{15}Ge_9C$. The main results are summarized in the conclusion section.

2. Experimental

2.1. Synthesis

The compounds were prepared by arc melting, in an inert atmosphere of argon, weighed amounts the rare earth (rod, 99.9 wt.% purity), germanium (piece, 99.999 wt.% purity) and carbon (6 mm-diameter rod, spectroscopic grade). Preferable route consisted in melting the R metal with C, to prepare first the corresponding carbide, and then melting together the parent carbide with germanium [3]; the alloys were turned upside-down and re-melted 3–4 times in order to ensure complete carbon dissolution and best homogenization. Total weight loss was lower than 0.5 wt.%, with no or negligible losses in C. The as-cast alloys, placed inside open out-gassed Ta crucibles and sealed under vacuum into quartz ampoules, were annealed at 1000 °C for 1 week, followed by a fast air-cooling. The samples were characterized by X-ray powder diffraction, using a Guinier camera, with pure Si as internal standard (a = 5.4308 Å) and Cu Kα1 radiation.

2.2. Neutron powder diffraction

Neutron diffraction data were collected on the *D1A* powder diffractometer at the Institut Laue Langevin using a wavelength of λ = 1.911 Å selected by the (1 1 5) reflection of a germanium crystal operating with a take-off angle of the monochromator of 122°. The high-resolution powder diffractometer *D1A* is unique in being able to provide high resolution at long wavelengths, with shorter wavelength contamination eliminated by the guide tube. *D1A* is particularly suited to study magnetic structures and other large *d*-spacing studies. Consequently, this was the optimal instrument for our study. In the configuration used the resolution of *D1A* is about 0.3° (*FWHM*) at 90°. During the neutron diffraction measurements a cylindrical vanadium sample holder of 6 mm inner diameter was used. The neutron detection is performed with 25 ^{3}He counting tubes spaced at 6°. The complete diffraction pattern is obtained by scanning the detectors in 2Theta. The FullProf Suite program was used for nuclear and magnetic structure refinements using the Rietveld method [4]; the agreement factors of the Rietveld refinement used are those as defined in Ref. [5].

3. Results and discussion

3.1. Crystallographic structures

To investigate the crystal structure of the $R_{15}Ge_9C$ carbides, neutron diffraction pattern were recorded at 100, 40 and 15 K for R = Nd, Pr and Ce respectively, *i.e.* above their magnetic transition temperature. One of the main goals was, in particular, to localize the carbon atoms in the structure, knowing that it contains three available octahedral cavities formed by the rare earth atoms. The three samples were nearly single phase: some amount of the secondary phase Ce_4Ge_3 was clearly visible in the Ce compound diffraction pattern as well as some traces of Pr_4Ge_3 for $Pr_{15}Ge_9C$. Apart from the binary impurity peaks, all reflections are well indexed with the space group $P6_3mc$ as reported previously [3] and with comparable unit cell parameters (Table 1). The lattice parameters obtained at low temperature from neutron diffraction are consistently smaller than those reported in [3] from room temperature X-ray diffraction analysis. The full refinements also confirm the superstructure of the Mn_5Si_3 structure type determined in previous results: it contains four inequivalent rare earth sites (one 12*d* and three 6*c* Wyckoff positions), three germanium sites (6*c*) and one site for the carbon atoms in 2*b* (1/3 2/3 ~0.5). However, while the above-mentioned 2*b* cavity is almost fully occupied in the three carbides, some doubts remain concerning the occupancy of the interstitial site 2*a* (0 0 ~0.5) by carbon atoms, as raised previously for the $R_{15}Si_9C$ silicides [12]. Indeed, for R = Ce and Pr, partial occupation of the 2*a* site of 36% and 33% respectively improves slightly the refinements and their agreement factors. It is worth to point out that an incomplete filling of interstitial site by carbon is not uncommon and has also been reported on other intermetallic compounds [6–8]. Concerning $Nd_{15}Ge_9C$ no significant improvement was observed with additional interstitial carbon in (0 0 ~0.5), letting some ambiguity on the localization of the carbon atoms in the Nd octahedrons. Besides, when the 2*a* (0 0 ~0.5) site is not accounted for in the refinement, the Fourier difference map does not clearly show additional nuclear density on this position, *i.e.*: the density is at the limit of the residual intensity background. If this site is taken into account in the refinement, its occupation rate is found to be around 30%. All crystal structure parameters for R = Ce, Pr and Nd are gathered in Table 1; the structure is depicted in Fig. 1.

The $R_{15}Ge_9C$ crystal structure is a superstructure of the Mn_5Si_3 type of the parent compounds ($a' = \sqrt{3}a$ and $c' = c$), the unit cell volume being three times larger than the R_5Ge_3 one. The $R_{15}Ge_9C$ structure results from a slight shift of the rare earth and germanium atoms in the parent structure in parallel to the ordered insertion of the carbon atoms [3]. The R atoms in the 6*c* site form infinite chains of trigonal antiprism (octahedra) along the *c*-axis and the Ge atoms connect these chains through the edges of the shared faces. The supercell possesses 6 octahedral cavities in 2*b* (1/3 2/3 ~0.5), 2*b* (1/3 2/3 ~0) and in 2*a* (0 0 0), but only the first 2*b* interstices are filled by carbon atoms along with the 2*a* ones but with a much smaller occupancy. It is interesting to note that the filled 2*b* cavities are considerably compressed compared to those in the parent compound. This suggests a strong covalent character of the R–C bonds and accounts for the significant change of the magnetic properties after C insertion due the modification of the R–R interactions within the octahedral chains. Thus, this confirms what was previously measured by means of X-ray diffraction and reported in Ref. [3]. In addition, the R–C interatomic distances in $Nd_{15}Ge_9C$ are found to be 2.56 and 2.58 Å against 2.55 Å and 2.76 Å for NdC_2 and Nd_2C_3 respectively. The Nd–C bonding in $Nd_{15}Ge_9C$ can be considered as short in such Nd environment

Table 1
Lattice and crystal structure parameters of the $Ce_{15}Ge_9C$, $Pr_{15}Ge_9C$ and $Nd_{15}Ge_9C$ compounds, as obtained from Rietveld refinement of the neutron diffraction data (λ = 1.911 Å).

Atom	$Ce_{15}Ge_9C$			$Pr_{15}Ge_9C$			$Nd_{15}Ge_9C$		
	x	*y*	*z*	*x*	*y*	*z*	*x*	*y*	*z*
R1 (12*d*)	0.0185(3)	0.3426(6)	0	0.0186(3)	0.3427(5)	0	0.0170(2)	0.3418(5)	0
R2 (6*c*)	0.4110(7)	2×	0.736(5)	0.4112(7)	2×	0.726(3)	0.4129(7)	2×	0.725(5)
R3 (6*c*)	0.2537(6)	2×	0.283(5)	0.2517(5)	2×	0.271(4)	0.2541(6)	2×	0.274(5)
R4 (6*c*)	0.0794(8)	2×	0.727(5)	0.0780(7)	2×	0.716(3)	0.0789(7)	2×	0.723(5)
Ge1 (6*c*)	0.1333(4)	2×	0.274(4)	0.1334(4)	2×	0.271(3)	0.1331(6)	2×	0.269(4)
Ge2 (6*c*)	0.4677(3)	2×	0.259(4)	0.4673(3)	2×	0.259(3)	0.4677(5)	2×	0.259(4)
Ge3 (6*c*)	0.1992(5)	2×	0.707(4)	0.1994(4)	2×	0.711(3)	0.2001(6)	2×	0.709(4)
C1 (2*b*)	1/3	2/3	0.506(9)	1/3	2/3	0.503(6)	1/3	2/3	0.500(6)
C2 (2*a*)	0	0	0.496(9)	0	0	0.498(6)	0	0	0.51(1)
Occ. C1	0.31(1)	93%		0.28(1)	84%		0.29(1)	87%	
Occ. C2	0.14(1)	36%		0.12(1)	33%		0.10(2)	30%	
a (Å)	15.3146(3)			15.2029(3)			15.1222(3)		
c (Å)	6.7611(2)			6.7449(2)			6.7028(2)		
R_{Bragg} (%)	6.3			7.7			8.7		

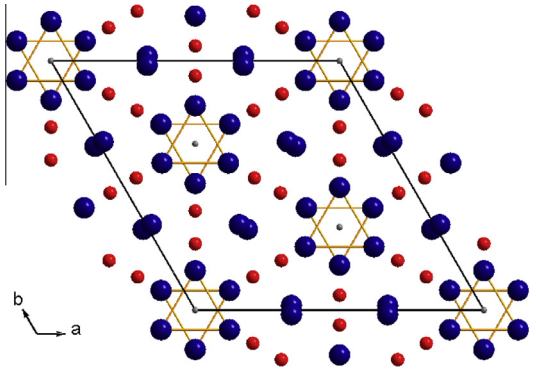

Fig. 1. Crystal structure of a $R_{15}Ge_9C$ compound viewed along the [001] direction. Rare earth atoms, germanium atoms and carbon atoms are depicted in blue, red and light grey (2*b* and 2*a* sites), respectively. (For interpretation of the references to color in this figure legend, the reader is referred to the web version of this article.)

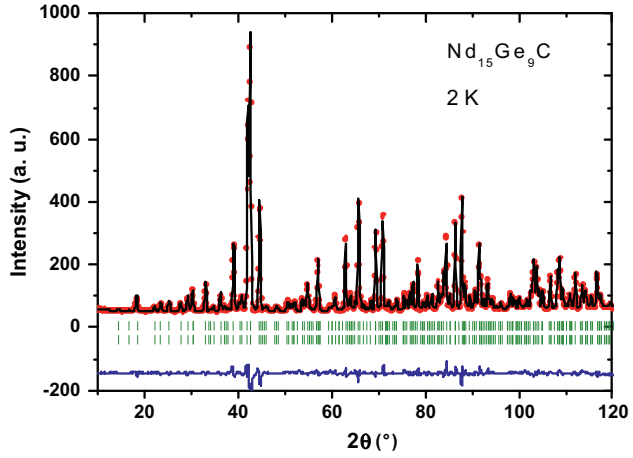

Fig. 2. Rietveld refinement plot of $Nd_{15}Ge_9C$ compound at 2 K.

and particularly strong. However shorter Nd–C bound of 2.49 Å may be observed in different environment as in $Nd_2Fe_{17}C_{0.7}$ [6,7].

3.2. Magnetic structure

3.2.1. $Nd_{15}Ge_9C$

According to magnetization measurements $Nd_{15}Ge_9C$ undergoes a ferromagnetic-like transition around T_C = 80 K [3]. Thus, to clarify the magnetic behavior of the Nd carbide, neutron diffraction patterns were recorded at 40, 20 and 2 K. Below the Curie temperature only existing Bragg peaks increase which is consistent with the ferromagnetic character of the carbide. These magnetic contributions indexed with the propagation vector **k** = [000] imply that the magnetic structure can be described within the nuclear cell. Symmetry analysis using magnetic group theory by means of BASIREPS program [9] was used to determine the magnetic structure. Considering the four inequivalent Nd sites, one in 12*d* and three in 6*c* Wyckoff positions, the space group $P6_3mc$ and the propagation vector **k** = [000], the analysis gives 6 allowed irreducible representations for both sites. Among the 6 irreducible representations (IR), five describe pure antiferromagnetic structures and only one contains basis vectors describing a mixed structure with a ferromagnetic component along the *c*-axis and an antiferromagnetic one within the (*a*–*b*) plane. Consequently, we choose this last IR solution to determine the magnetic structure of $Nd_{15}Ge_9C$, in accordance with its magnetic properties. Using this model we obtain a good refinement of the neutron data at 2 K. The final refinement and the corresponding magnetic structure are shown in Figs. 2 and 3 respectively. This magnetic structure can be seen as a canted ferromagnetic type structure with a main ferromagnetic component along the *c*-axis. The antiferromagnetic component corresponds to an arrangement of the moments at 120° from each other within the hexagonal basal plane for each Nd site. The details of this magnetic structure are given in Table 2. Note that the low accuracy of the values arises from the large number of refined parameters with respect to the low magnetic contribution to the total scattering.

It is worth mentioning that Nd1 and Nd4 almost have a pure ferromagnetic configuration (θ_1 = 10(3)° and θ_4 = 6(7)°) while Nd2 and Nd3, close to the C1 carbon atom, are more canted since θ_2 = 30(8)° and θ_3 = 45(5)°. This indicates a very low antiferromagnetic coupling of the Nd1 and Nd4 moments within the basal plane and a stronger one for the Nd2 and Nd3 moments. The average Nd moment is found equal to 2.2 μ_B but the value for Nd3 (3.0 μ_B) is significantly larger than those for Nd1, Nd2 and Nd3 which are close to 2 μ_B/Nd. The mean magnetic moment is weaker than the free ion value *gJ* = 3.27 but higher than the value determined for the parent compound Nd_5Ge_3 by means of neutron diffraction experiment, namely 1.36 μ_B from Ref. [10] or 0.66 μ_B from Ref. [11]. These reduced moments may reasonably be ascribed to crystal electric field effects as it was assumed for the parent compound Nd_5Ge_3.

With increasing temperature, the model using the chosen IR is still valid to refine the neutron data, providing the evolution of the magnetic moment on each site (Fig. 4). In particular, although the limited number of temperatures, we observe that the moment on Nd1 increases and saturates rapidly below T_C. The different thermal behavior for Nd2, Nd3 and Nd4 can be ascribed to different structural environments around these atoms which belong to octahedrons chains unlike Nd1.

The magnetic structure of $Nd_{15}Ge_9C$ presents strong similarities with its isotypic homologous $Ho_{15}Si_9C$ [12]. Notably, the neutron diffraction data disclose similar magnetic couplings of the four different rare earth sites with respect to the *c*-axis and the (*a*–*b*) plane. The temperature dependence of the Nd1 moment, which saturates rapidly compared to the 3 other Nd atoms, was also previously mentioned for Ho1.

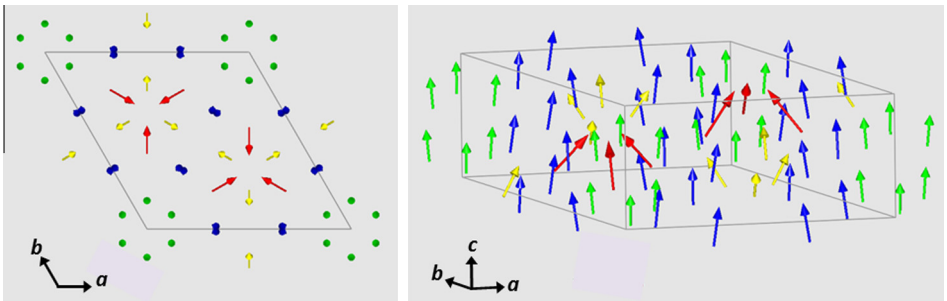

Fig. 3. Magnetic structure of $Nd_{15}Ge_9C$: view along *c*-axis (left) and 3D view (right).

Table 2
Magnetic structure parameters of the $R_{15}Ge_9C$ carbides obtained from Rietveld refinement of the neutron diffraction data at 2 K (λ = 1.911 Å). μ_{tot}, μ_F (μ_{AF}) and θ are the total magnetic moment, the ferromagnetic (antiferromagnetic) component of the moment and the canting angle relative to the *c*-axis, respectively.

	$Ce_{15}Ge_9C$		$Pr_{15}Ge_9C$			$Nd_{15}Ge_9C$		
	μ_{tot} (μ_B)	θ (°)	μ_{AF} (μ_B)	μ_F (μ_B)	θ (°)	μ_{tot} (μ_B)	μ_F (μ_B)	θ (°)
R1 (12*d*)	1.10(7)	97(5)	1.13(8)	1.72(5)	118(5)	2.10(5)	2.07(4)	10(3)
R2 (6*c*)	0.7(2)	50(20)	0.4(1)	1.4(2)	76(21)	2.0(4)	1.7(3)	30(8)
R3 (6*c*)	0.7(2)	36(20)	0.7(1)	1.5(3)	120(10)	3.0(3)	2.2(3)	45(3)
R4 (6*c*)	0.8(2)	36(12)	1.9(1)	1.1(2)	−64(4)	1.9(5)	1.9(5)	6(7)
a (Å)	15.3139(3)		15.2015(3)			15.1081(3)		
c (Å)	6.7616(2)		6.7450(2)			6.7053(2)		
$R_{B\text{-nuc}}$ (%)	6.3		6.7			6.9		
$R_{B\text{-mag}}$ (%)	12.5		13.2			8.5		

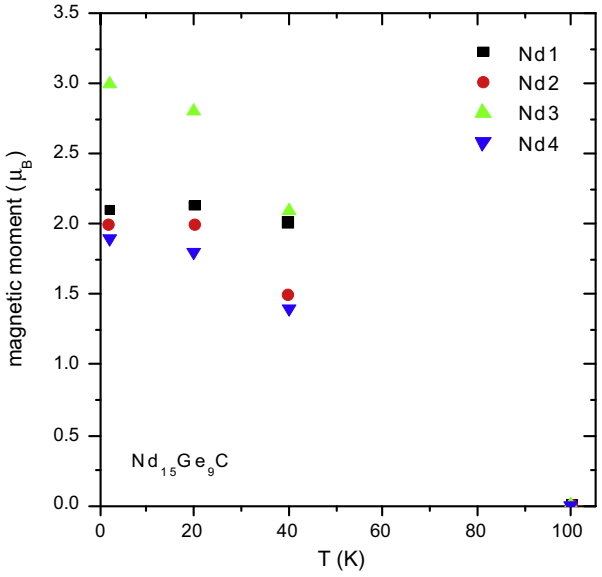

Fig. 4. Temperature dependence of the Nd magnetic moments in $Nd_{15}Ge_9C$.

3.2.2. $Pr_{15}Ge_9C$ and $Ce_{15}Ge_9C$

Magnetic structures of $Pr_{15}Ge_9C$ and $Ce_{15}Ge_9C$ were determined at low temperature. Magnetization measurements have shown that both carbides exhibit a ferromagnetic type transition at 30 K and 9 K for $Pr_{15}Ge_9C$ and $Ce_{15}Ge_9C$, respectively. The neutron diffraction patterns at 2 K are shown in Fig. 5; they present many similarities with that of the Nd carbide. In particular, the magnetic contributions are again indexed with the propagation vector **k** = [000], allowing us to make use of the same magnetic symmetry analysis as for $Nd_{15}Ge_9C$. Therefore, in agreement with their magnetic properties, we chose the same IR as for the Nd carbide to determine their magnetic structures.

This model accounts well for the magnetic contributions of the Ce compound. The refinement was performed on the difference pattern "2 K–15 K" to increase the sensitivity to the weak magnetic contribution. Besides, the magnetic moment values of Ce2 and Ce3 were constrained to be equal to help the convergence of the fit. The result is reported in Fig. 5 on the whole pattern at 2 K and the parameters summarized in Table 2. Note that the nuclear and magnetic contributions of the impurity Ce_4Ge_3 has been included in the refinement. The magnetic structure of the binary compound has been solved and referred in Ref. [13]. It corresponds to a commensurate antiferromagnetic structure with Ce spins directed up and down along the *c*-axis. For the carbide $Ce_{15}Ge_9C$, the determination of the magnetic structure is hampered by the low values of the Ce moments. However, the small mean value of 0.9 μ_B/Ce is consistent with the magnetization data M(H) performed at 2 K which also

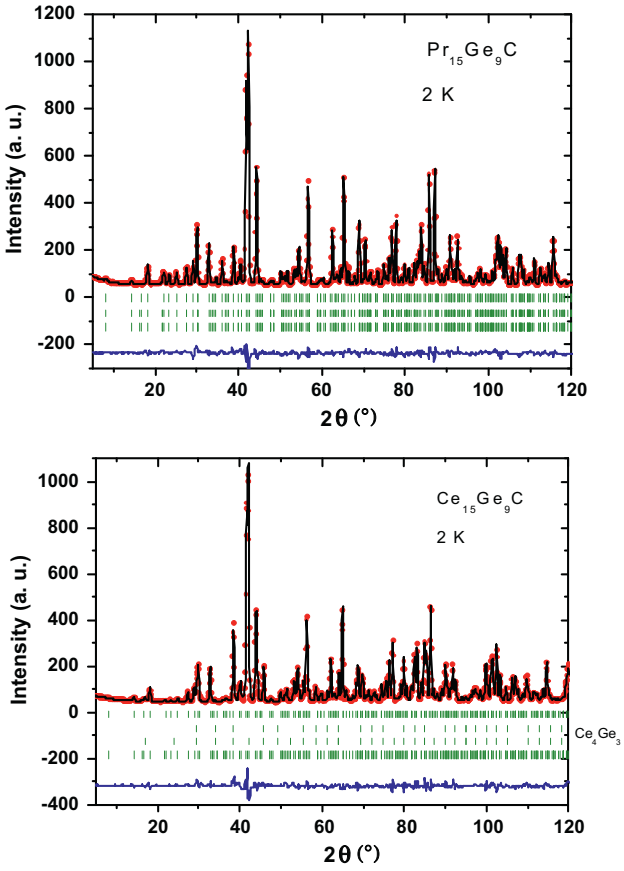

Fig. 5. Rietveld refinement plots of the $Pr_{15}Ge_9C$ and $Ce_{15}Ge_9C$ compounds at 2 K. For the Ce carbide the nuclear and magnetic contributions of the Ce_4Ge_3 impurity is added.

indicate a non-pure ferromagnetic ground state. Besides, these low values with respect to the free ion Ce^{3+} value strongly support the Kondo behavior stated previously from resistivity and specific heat data [3]. Such values were also found for the parent Kondo compound Ce_5Ge_3 [14]. However, if this study is in fair agreement with the previous physical investigations, it cannot provide explanations about the transition around 4 K clearly visible on the heat capacity curve and assigned to re-orientation of magnetic moments.

Concerning $Pr_{15}Ge_9C$, the model of magnetic structure used previously for the Nd and the Ce isotypes do not correctly fit the neutron data. Indeed, the best refinement obtained with this irreducible representation ($R_{B\text{-mag}}$ = 18.5%) exhibits many discrepancies between the observed and the calculated intensities, in particular on the reflections (112), (220) and (221). Moreover, all the other allowed IR, with antiferromagnetic couplings only,

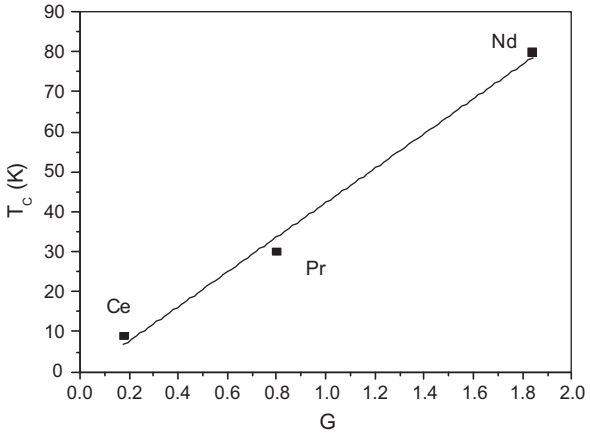

Fig. 6. Magnetic ordering temperature *vs*. de Gennes factor G for the $R_{15}Ge_9C$ carbides.

were tested and did not yield a better fit of the measured intensities. We assume that this incorrect fit cannot arise from the impurity Pr_5Ge_3 since no magnetic reflection is observed in neutron data down to 2 K in zero magnetic field [11]. On the other hand, we obtain a much better fit of the data if we include the ferromagnetic component within the (*a*–*b*) plane. However, its direction remains undetermined due to the equivalence of the reflections in powder diffraction. Eventually, the best fit of the neutron data is obtained by including this ferromagnetic component into the basal plane and an antiferromagnetic one given by the symmetry analysis. The refined parameters of the fit are detailed in Table 2. Again, the low accuracy arises from the weak magnetic moment values.

This result points out a conflict with the symmetry analysis giving no IR with a ferromagnetic contribution within the basal plane. This is usually observed if the symmetry is actually lower than the apparent one, which may occur in case of a slight distortion of the unit cell breaking the hexagonal symmetry for example. But we cannot know whether there are two separated phases into the sample, each one having its own magnetic structure or only one phase with a lower symmetry. In order to check carefully the symmetry of the phase(s) it would be useful to perform electron microscopy and/or synchrotron measurements on the $Pr_{15}Ge_9C$ sample.

It is interesting to notice that the same problem was also evidenced for the $Tb_{15}Si_9C$ carbide [12]. The synchrotron data [12] indicated a structural change *via* the broadening or the splitting of some peaks and the authors supposed the coexistence of an antiferromagnetic hexagonal phase and a ferromagnetic phase with a lower symmetry. Some magnetization measurements on $Pr_{15}Ge_9C$ single crystals would also be helpful to clarify the magnetocrystalline anisotropy.

It is worth to note that a ferromagnetic correlations within the hexagonal plane of the parent compound Pr_5Ge_3 was also reported on single crystal magnetization measurements, although a ferromagnetic transition along the *c*-axis at lower temperature [15]. The (*a*–*b*) plane was found to be the easy magnetization plane.

Finally, a comparison of the ordering temperature for the three studied $R_{15}Ge_9C$ compounds reveals that the T_C varies linearly with the de Gennes factor of the rare-earth (Fig. 6). This result confirms the importance of RKKY interactions and bears witness to the trivalent character of Ce in this $R_{15}Ge_9C$ compound since it behaves similarly to the Pr and Nd isotypic phases.

4. Conclusion

The interstitial carbon atoms occupy mainly the Wyckoff site 2*b* in the position (1/3 2/3 ~1/2) and also, with a smaller occupancy rate, the Wyckoff site 2*a* at (0 0 ~1/2) for R = Ce and Pr. The reduction of the filled cavity dimension suggests an increase of the covalent character of the R–C bonds.

In the magnetic state, the three compounds display canted ferromagnetic structures with a propagation vector **k** = [0 0 0].

The magnetic structures of these $R_{15}Ge_9C$ compounds strongly differ from those of their parent R_5Ge_3 germanides (being these mainly antiferromagnetic), but present strong similarities with those of $R_{15}Si_9C$ compounds [12]; the overall results indicating the drastic influence of insertion of carbon atoms in the rare earth environment via the R octahedral distortion and R–C bonding which modifies strongly the RKKY interactions. Therefore, ordering temperatures, magnetic moment values and magnetic structures are changed by carbon insertion.

Further search on the $Pr_{15}Ge_9C$ compound, as magnetization measurements performed on single crystal or supplemental data from synchrotron, would be useful to clarify the magnetic structure of this compound.

References

[1] A.M. Guloy, J.D. Corbett, Inorg. Chem. 35 (1996) 4669.
[2] F. Wrubl, PhD Thesis, University of Genova, Italy, 2012.
[3] F. Wrubl, K.V. Shah, D.A. Joshi, P. Manfrinetti, M. Pani, C. Ritter, S.K. Dhar, J. Alloys Comp. 509 (2011) 6509.
[4] J. Rodriguez-Carvajal, Physica B 192 (1993) 55.
[5] L.-B. McCusker, R.-B. Von Dreele, D.-E. Cox, D. Louër, P. Scardi, J. Appl. Cryst. 32 (1999) 36.
[6] X.P. Zhong, R.J. Radwanski, F.R. de Boer, T.H. Jacobs, K.H.J. Buschow, J. Magn. Magn. Mater. 86 (1990) 333.
[7] O. Isnard, J.L. Soubeyroux, D. Fruchart, T.H. Jacobs, K.H.J. Buschow, J. Alloys Comp. 186 (1992) 135.
[8] O. Isnard, PhD Thesis, Université J. Fourier, France, 1993.
[9] J. Rodriguez-Carvajal, Satellite Meeting, in: 15th IUCr Congress on Powder Diffaction, Toulouse, 1990, p. 127.
[10] P. Schobinger-Papamentellos, J. Magn. Magn. Mater. 49 (1985) 349.
[11] R. Nirmala, A.V. Morozkin, A.K. Nigam, J. Lamsal, W.B. Yelon, J. Appl. Phys. 109 (2011) 07A716.
[12] C. Ritter, F. Wrubl, A.H. Hill, M. Pani, P. Manfrinetti, J. Phys.: Condens. Matter. 23 (2011) 296002.
[13] A.V. Morozkin, O. Isnard, R. Nirmala, S.K. Malik, J. Alloys Comp. 486 (2009) 497.
[14] M. Kurisu, T. Mitsumata, I. Oguro, Physica B 259 (1999) 96.
[15] D.A. Joshi, A. Thamizhavel, S.K. Dhar, Phys. Rev. B 79 (2009) 014425.